Heat Mass Transfer (2007) 44:175–186
DOI 10.1007/s00231-007-0232-0

ORIGINAL

Convective heat transfer characteristics of microencapsulated phase change material suspensions in minichannels

Yu Rao · Frank Dammel · Peter Stephan · Guiping Lin

Received: 30 May 2006 / Accepted: 13 December 2006 / Published online: 17 February 2007

Abstract A comparative experimental study was conducted in order to investigate the convective heat transfer characteristics of water-based suspensions of microencapsulated phase change material (MEPCM) flowing through rectangular copper minichannels. The hydraulic diameter of the channels was 2.71 mm. MEPCM particles with an average size of 4.97 μm were used to form suspensions with mass concentrations ranging from 0 to 20%. The comparative experiments were performed for varying mass flow rates in the laminar region and varying thermal conditions. The cooling performance of the MEPCM suspensions strongly depended on the mass flow rate and the MEPCM mass concentration. The 5% suspension always showed a better cooling performance than water resulting in lower wall temperatures and enhanced heat transfer coefficients within the whole range of mass flow rates. The suspensions with higher mass concentrations, however, were more effective only at low mass flow rates. At higher mass flow rates they showed a less effective cooling performance than water.

Y. Rao · F. Dammel · P. Stephan (✉)
Technical Thermodynamics,
Darmstadt University of Technology,
Darmstadt, Germany
e-mail: pstephan@ttd.tu-darmstadt.de

F. Dammel
e-mail: dammel@ttd.tu-darmstadt.de

Y. Rao · G. Lin
Department of Aeronautical Science and Engineering,
Beihang University, Beijing 100083
People's Republic of China
e-mail: yuraohello@yahoo.com

List of symbols

A	Total area of channel bottom and side walls (m^2)
c	Mass concentration of MEPCM in the fluid
c^*	Volume concentration of MEPCM in the fluid
C	Specific heat (J/kg K)
d	Diameter (m)
D_h	Hydraulic diameter (m)
h	Heat transfer coefficient (W/m^2 K)
H_{ch}	Height of a minichannel (m)
H_{w2}	Distance between thermocouple position and channel bottom wall (m)
I	Total electrical current supplied to heaters (A)
k	Thermal conductivity (W/m K)
M	Mass flow rate of the fluid (kg/s)
N	Total number of minichannels
Nu	Nusselt number
q_0	Heat flux at thermocouple position from below (W/m^2)
Q	Total electrical heating power (W)
T_{in}	Inlet temperature (°C)
T_{out}	Outlet temperature (°C)
T_{tci}	Thermocouple reading (i = 1–6) (°C)
T_{wi}	Channel bottom wall temperature (i = 1–6) (°C)
ΔT_m	Mean temperature difference between fluid and channel bottom wall (°C)
U	Electrical voltage at heaters (V)
W_{ch}	Width of a minichannel (m)

Greek symbols

ρ	Density (kg/m^3)
μ	Viscosity (kg/m s)

Subscripts

b	Bulk
cb	Copper block
p	MEPCM particle
mc	MEPCM core
ms	MEPCM shell
w	Water

1 Introduction

The use of microencapsulated phase change material (MEPCM) suspensions as heat transfer fluid has attracted more and more interest since about two decades due to their capability of enhancing convective heat transfer and thermal storage performance [1–9]. This heat transfer enhancement results from the latent heat absorption by the PCM in the suspended MEPCM particles during the melting process, the tremendously increased surface area per unit volume due to the microminiaturization of PCM and the interaction of MEPCM particles in the fluid.

Previous studies on convective heat transfer of MEPCM suspensions, performed both experimentally and theoretically, showed that, compared with single phase fluids, MEPCMs can enhance convective heat transfer performance resulting in appreciable reduction in mass flow rate, wall temperature and pumping power [1–9]. Kasza and Chen [1] performed a theoretical evaluation on the benefits of using PCM slurries. Their performance study indicated that, compared with a system using a conventional single phase working fluid, the source to sink temperature difference, mass flow, pumping power and storage volume requirements can be significantly reduced by using PCM slurries, while achieving a threefold or greater heat transfer enhancement for certain heat transfer surface geometries. Yamagishi et al. [2] investigated the structural integrity of MEPCM and the rheological properties of MEPCM-water suspensions. They showed that smaller particles (5~10 μm) of MEPCM could better withstand the stress from the suspension flow and the volumetric expansion due to phase change. Goel et al. [3] studied the laminar forced convective heat transfer performance of a MEPCM-water suspension flowing in a circular tube with various MEPCM volume concentrations from 0 to 20%. In their study, they analyzed the effects of Stefan number, volume concentration and particle size on the heat transfer performance by conducting comparative experiments at the same Reynolds number. Compared with water, they observed a significant reduction in wall temperature rise of up to 50% for MEPCM suspensions. More recently, Inaba et al. [4] examined the laminar and turbulent heat transfer characteristics of a 20 mass% MEPCM suspension with particles of different sizes flowing in a circular tube with constant wall heat flux. They revealed that the average heat transfer coefficients of the MEPCM suspension flows were 2–2.8 times greater than those of pure water flow at the same Reynolds number. In the turbulent flow region, the friction factor of the slurry was found to be lower than that of pure water due to the drag reducing effect of the particles. Studies on natural convection in MEPCM suspensions or PCM slurries were conducted by Datta et al. [8] and Inaba et al. [9]. Datta et al. [8] reported an up to 80% increase in heat transfer for MEPCM concentrations up to 5%. For higher concentrations they found that the heat transfer was reduced due to agglomeration and settling effects of particles. Inaba et al. [9] used PCM slurries and showed that the phase change phenomenon of the suspended PCM enhanced the heat transfer in natural convection.

It should be pointed out that most of the previous research on heat transfer or flow characteristics of MEPCM suspensions was focused on flows in macrochannels ($D_h > 5$ mm), mostly in circular tubes. The heat transfer performance of the MEPCM suspensions was usually compared to that of the single phase base fluid at the same Reynolds number [3–7]. Those researchers based the Reynolds number on the suspension's viscosity, which was developed from viscosity correlations. For dilute suspensions with a particle concentration of less than 5 vol.% accurate correlations are available. However, for more concentrated suspensions, which contain micro sized particles with a wide size distribution and a non-smooth particle surface, it is difficult to estimate the viscosity with reliable accuracy [10–14], and there may be considerable errors up to ca. 50% using these viscosity correlations. The errors of the suspension's viscosity propagate directly to the Reynolds number. On the other hand, since the viscosity of the fluid is increased considerably by dispersing MEPCM particles in it, the suspension's velocity and thus its mass flow rate is considerably higher than that of the pure base fluid at the same Reynolds number. Correspondingly, the pumping power is also considerably higher. Therefore, it is difficult to determine to what extent the enhancement in heat transfer is due to phase change and particle interaction in the MEPCM suspension flow, and thus it is also difficult to judge whether the MEPCM suspension is really superior compared to the single phase base fluid as a coolant.

In the present study, comparative experiments were conducted under the same mass flow rates and thermal

conditions using water and water-based MEPCM suspensions with various MEPCM mass concentrations from 5 to 20%, which flow in three parallel rectangular minichannels (hydraulic diameter D_h = 2.71 mm). The mass flow rates ranged from 0.05 to 0.35 kg/min, providing laminar flow in the three parallel minichannels with mass flux densities from 33.1 to 231.5 kg/m^2 s. The heat transfer characteristics were examined by investigating the effects of MEPCM mass concentration and mass flow rate on wall temperatures and heat transfer performance.

2 Physical properties of MEPCM and MEPCM suspensions

As shown in Fig. 1, a single MEPCM particle consists of two parts: the outer polymer shell and the inner phase change material. The Scanning Electron Microscope (SEM) photo of the MEPCM in Fig. 2 shows particles which have a size that ranges from 1 to 5 μm. The investigated MEPCM particles have an average size of 4.97 μm. The core material is *n*-Octadecane, which has a melting temperature of about 28°C, and the shell material is Polymethylmethacrylat (PMMA). The mean mass concentration of the core material (PCM) in a single MEPCM particle is about 80.9%. Due to the tiny size of the MEPCM particles, a density close to that of the carrier fluid (water) and due to the presence of a dispersant in the suspension, the MEPCM can be homogeneously dispersed in the fluid.

The bulk suspension properties are a combination of the properties of the base fluid and the MEPCM particles. Table 1 shows the relevant thermodynamic and hydrodynamic properties of the suspension components and the suspensions. The properties of the components were taken from literature (see Table 1) and shall represent constant mean values in the relevant temperature range in this study. The bulk suspension values were determined as explained in the following paragraphs. The bulk density of the suspension, ρ_b, is given by

$$\rho_b = \rho_w \cdot (1 - c^*) + \rho_p \cdot c^*, \tag{1}$$

where c^* is the volumetric concentration of the MEPCM and ρ_w and ρ_p the densities of water and MEPCM particles, respectively. The density ρ_p is calculated from the densities of *n*-Octadecane and PMMA according to their volumetric fractions in the particle.

The bulk suspension specific heat, C_b, is calculated by

$$C_b = C_w \cdot (1 - c) + C_p \cdot c, \tag{2}$$

where c is the mass concentration of MEPCM and C_w and C_p the specific heats of water and MEPCM particles, respectively. The specific heat C_p is calculated from the specific heats of *n*-Octadecane and PMMA according to their mass fractions in the particle.

The bulk suspension thermal conductivity, k_b, is calculated according to Maxwell's correlation [3, 4]:

$$\frac{k_b}{k_w} = \frac{2 + \frac{k_p}{k_w} + 2c^*\left(\frac{k_p}{k_w} - 1\right)}{2 + \frac{k_p}{k_w} - c^*\left(\frac{k_p}{k_w} - 1\right)}, \tag{3}$$

with the thermal conductivities k_w of water and k_p of the MEPCM particles. The bulk suspension conductivity k_b is the thermal conductivity of the static suspension. For a flowing suspension, some researchers

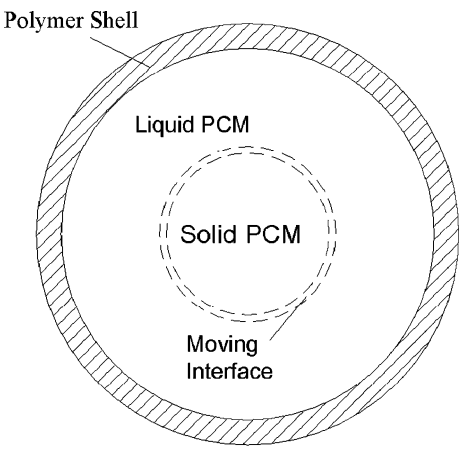

Fig. 1 Sketch of a single MEPCM particle during melting

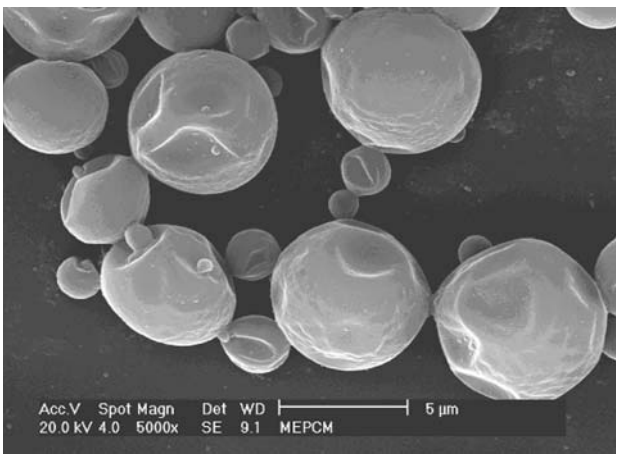

Fig. 2 MEPCM SEM photo

Table 1 Physical properties of suspension components and suspensions

	Density (kg/m^3)	Specific heat (J/kg K)	Thermal conductivity (W/m K)	Viscosity (kg/m s)	Latent heat (kJ/kg)
Water	997	4,180	0.604	1.0×10^{-4}	–
n-Octadecane [15] (MEPCM core)	850 (solid) 780 (liquid)	2,000	0.18	–	241
PMMA [16] (MEPCM wall)	1,190	1,470	0.21	–	–
MEPCM particle	867.2[a]	1,899	0.1643	–	–
5% suspension	989.6	4,065	0.571	See Table 2	–
10% suspension	982.3	3,951	0.541	See Table 2	–
20% suspension	968	3,723	0.483	See Table 2	–

[a] Density of PCM used here is the mean of its solid and liquid densities

[17, 18] used an effective thermal conductivity considering the microconvection caused by the suspended particles. Such an effective thermal conductivity is closely related to the relative velocity between particles and carrier fluid and thus depends on the position in the channel. Therefore, a Nusselt number based on the conductivity k_b of the static suspension is used here.

The particle conductivity k_p was calculated using the method described in Ref. [3]:

$$\frac{1}{k_p d_p} = \frac{1}{k_{mc} d_{mc}} + \frac{d_p - d_{mc}}{k_{ms} d_p d_{mc}}, \tag{4}$$

with the thermal conductivities k_{mc} of the MEPCM core material and k_{ms} of the shell material, the particle diameter d_p and the MEPCM core diameter d_{mc}.

Two methods were investigated to determine the bulk viscosity μ_b of the suspension:

1. Calculating the bulk viscosity using Vand's correlation [10] as suggested also by other authors [3, 4]:

$$\frac{\mu_b}{\mu_w} = (1 - c^* - 1.16c^{*2})^{-2.5}, \tag{5}$$

where μ_w is the dynamic viscosity of water.

2. Measuring the bulk viscosity with a cylindrical rotating rheometer.

Table 2 shows the bulk viscosities calculated from the correlation (Eq. 5) and measured by the rheometer. The agreement of the two values gets worse with increasing particle concentration. For 5% MEPCM mass concentration Vand's correlation underpredicts the measured value by 9.7%. For 10 and 20% mass concentration the difference increases to 40 and 54.4%, respectively. Vand extended Einstein's correlation, which is valid for infinitely diluted suspensions of rigid spheres, to higher concentrations. However, a spherical shape of the particles is still required.

The deviations of the MEPCM particles' shape from rigid spheres, visible in Fig. 2, seems to be the main reason for the poor agreement between correlation and measurement.

To characterize different phase transitions in the MEPCM over a given temperature range, a thermal analysis was performed using a Differential Scanning Calorimetry (DSC 821^e Module, Mettler Toledo Star^e System). Both heating and cooling processes were applied to a certain amount of dried MEPCM particles to examine the onset temperature, endset temperature and the enthalpy of the phase change in the MEPCM. The temperature program was as follows. In the heating process the temperature starts from 10°C and increases up to 40°C at a heating rate of 2°C/min. In the cooling process the temperature decreases from 40°C down to 10°C at a cooling rate of 2°C/min. Figure 3 shows the results of the DSC thermal analysis. The temperature range of the MEPCM during the melting is in between the onset temperature of 24°C and the endset temperature of 29°C. Figure 3 also shows that, compared with the solid–liquid phase change temperature in the heating process, there is a hysteresis of about 4.6°C in the liquid–solid phase change temperature of the PCM in the cooling process, which is due to the subcooling phenomena in the freezing process of the PCM. On the other hand, a second peak appeared in the cooling process, which indicates that different nucleation processes (heterogeneous and homogeneous) might have occurred in the PCM crystallization process as reported by [2]. An approximate value of

Table 2 Bulk viscosities of MEPCM suspensions

MEPCM mass concentration (%)	Bulk viscosity from Vand's correlation (kg/m s)	Bulk viscosity measured by rheometer (kg/m s)
5	1.147×10^{-3}	1.27×10^{-3}
10	1.38×10^{-3}	2.3×10^{-3}
20	2.233×10^{-3}	4.9×10^{-3}

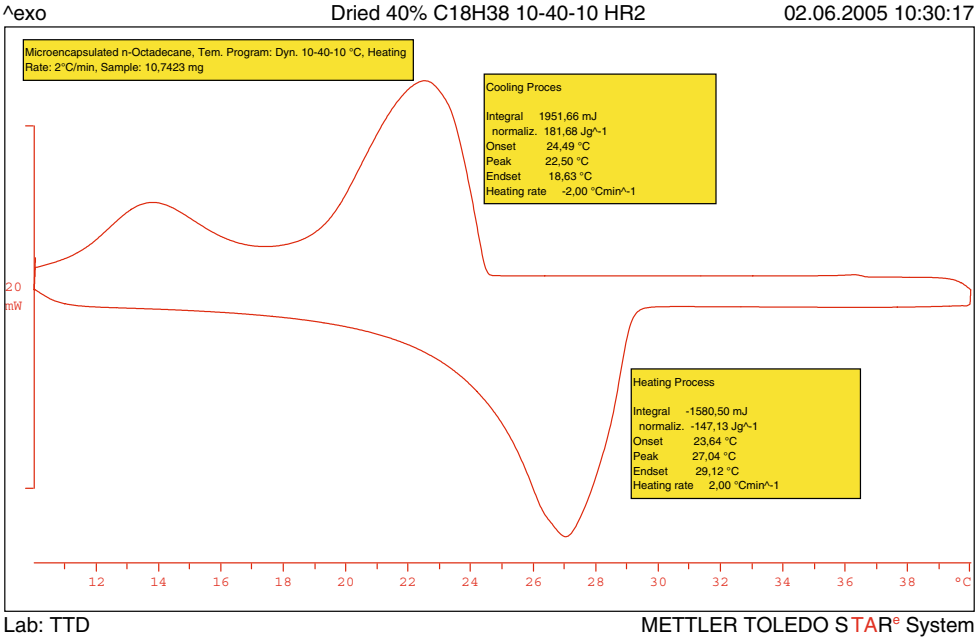

Fig. 3 DSC thermal analysis of dried MEPCM particles

the melting enthalpy of MEPCM between 24 and 29°C can also be obtained from Fig. 3, i.e., 147.1 kJ/kg, which is lower than the freezing enthalpy of about 181.7 kJ/kg between 24.5 and 18.6°C. Such a difference in enthalpy values is believed to be mainly caused by manually selecting the temperature range of interest for the heating and cooling process in the data analysis using the provided software, and also by the big errors in measurement when the temperature approaches the coldest point achievable by the used cooling thermostat. A more detailed discussion on the DSC measurement is not made here, since it is out of the focus of this paper.

The hysteresis prescribes the necessary temperature range in a technical application. With increasing temperature difference between the highest and the lowest temperature in a cooling cycle with MEPCM suspension as working fluid the percentage of the total heat that is stored as latent heat decreases. Therefore, it would be beneficial to find measures—e.g., in the manufacturing process—to reduce this hysteresis effect.

3 Experimental set-up

3.1 Flow loop

To investigate both flow and heat transfer characteristics of the MEPCM-water suspensions flowing through minichannels, the flow loop illustrated in Fig. 4 was constructed and built. It consists of a test section with heated minichannels (see Chap. 3.2), a flow meter, a damper, a preheating plate heat exchanger, a post-cooling plate heat exchanger, a thermostat, a reservoir, a peristaltic pump and adjusting valves. The MEPCM suspension was pumped from the reservoir using the peristaltic pump and circulated through the flow loop. Leaving the pump, the suspension passed by the damper, which could reduce the pulsation in the flow caused by the pump, then flowed through a preheating heat exchanger which was connected to a temperature controlled thermostat, so that the inlet temperature of the test section could be precisely adjusted to a predetermined temperature. Leaving the test section, the suspension flowed through the post-cooling heat exchanger, which is connected with a cooling thermostat to cool down the fluid to a temperature always below 6°C in order to re-solidify any PCM before returning to the reservoir. The flow rate of the suspension that entered the test section was measured by a Coriolis flow meter and controlled by adjusting the valves installed in both the test loop and the bypass line.

3.2 Test section

Figure 5 illustrates the construction of the test section, which consists of a minichannel heat sink made of oxygen-free copper, a ceramic fiber insulating housing with a bottom plate, a transparent polycarbonate cover plate, 18 cylindrical cartridge heaters placed inside the copper block and flow inlet and outlet tubes. At the top of the copper block, between the inlet and outlet ports,

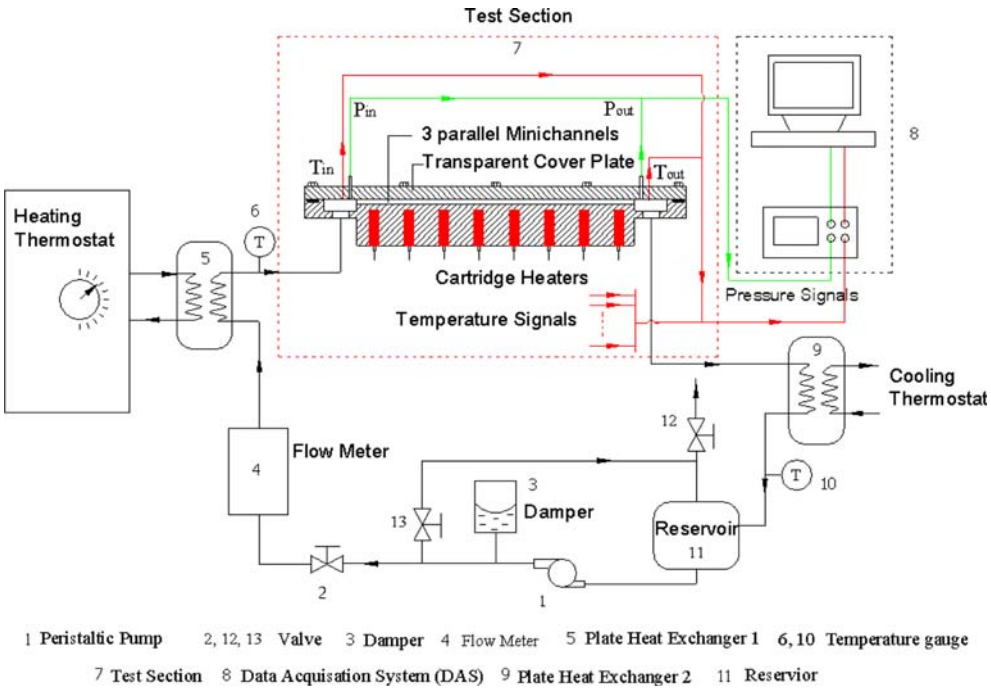

Fig. 4 Scheme of the MEPCM suspension flow loop

three rectangular 2 mm wide and 4.2 mm deep minichannels were machined, each 150 mm in length. The channels and inlet and outlet ports were configured in such a way that the mass flow through the channels was uniformly distributed. This was confirmed by a three-dimensional simulation with the commercial CFD code Fluent taking into account the entire geometry of the inlet port, the three parallel channels and the outlet port. Below the channel bottom surface six Type-K thermocouples were placed along the center plane to measure the heat sink's stream-wise temperature distribution. Eighteen holes were drilled into the copper block from its bottom to accommodate the cartridge heaters. These cartridge heaters were powered by a 0–230 V AC transformer, and their total electrical power was obtained by measuring the supplied AC voltage and current with a precision ammeter.

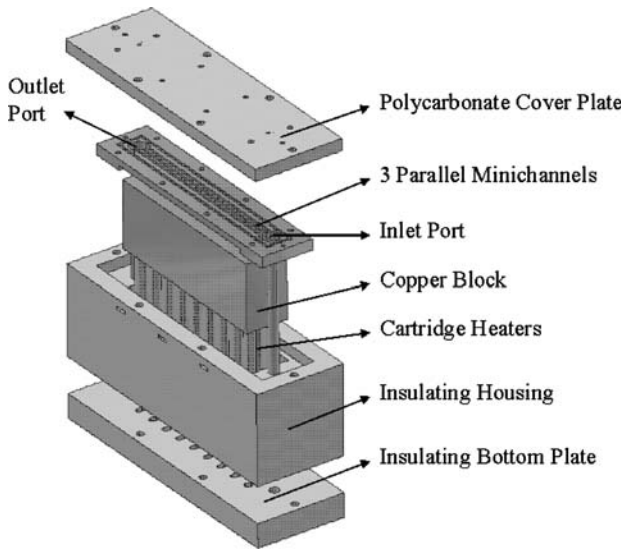

Fig. 5 Construction of the test section

The transparent cover plate, which was bolted from the top to form the minichannels, facilitated direct visual access to the flowing suspension. At the ports upstream and downstream, two pressure taps and two Type-K thermocouples were mounted through the cover plate for inlet and outlet pressure and temperature measurement, respectively. The whole copper heat sink was inserted into a ceramic-fiber thermal insulating housing, and the heat sink was also insulated at the bottom by a ceramic fiber plate. To reduce the heat loss to the ambient, the whole ceramic fiber block was wrapped with rock wool. Figure 6 shows the cross section of the test section with the three minichannels and the cover plate.

4 Data reduction and error analysis

4.1 Average heat transfer coefficient

In this paper, the average heat transfer coefficient for MEPCM suspensions flowing through rectangular minichannels is defined by

$$h = \frac{Q}{NA\Delta T_m}. \tag{6}$$

The heat transfer area A contains the side walls and the bottom wall of a channel, but not the polycarbonate top plate which is assumed to be adiabatic. The number of the parallel channels is $N = 3$. The total electric heating power Q is obtained by multiplying the voltage value by the current value, which is

$$Q = UI. \tag{7}$$

The mean temperature difference ΔT_m between the wall and the fluid is evaluated by [19]

$$\Delta T_m = \frac{1}{6}(T_{w1}+T_{w2}+T_{w3}+T_{w4}+T_{w5}+T_{w6}) - \frac{1}{2}(T_{in}+T_{out}), \tag{8}$$

where T_{in} is the mean inlet and T_{out} the mean outlet temperature of the fluid. The wall temperatures T_{w1}, T_{w2}, ...,T_{w6} of the channel bottom are calculated, as shown in Fig. 6, by assuming one-dimensional heat conduction in the copper block underneath the minichannels [20]. This leads to

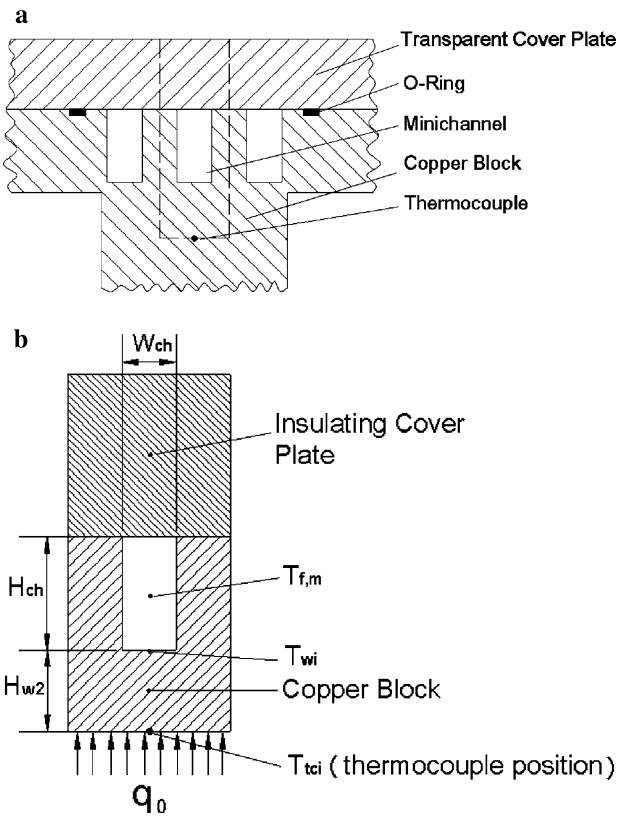

Fig. 6 Cross section of the minichannels

$$T_{wi} = T_{tci} - \frac{q_o H_{w2}}{k_{cb}}, \tag{9}$$

where the temperatures T_{tci} (i = 1, ..., 6) are the values measured by the thermocouples, H_{w2} is the distance between the thermocouples and the channel bottom wall, k_{cb} is the thermal conductivity of the copper block, and q_0 is the mean heat flux. The mean heat flux is calculated by dividing the total heating power (Eq. 7) by the cross sectional area at the thermocouple position in the copper block. Due to thermal conduction in the copper block the heat flux is slightly higher than this mean value near the inlet port where the cold suspension enters the channels. Correspondingly, the heat flux is lower than the mean value near the outlet port. Because of this effect the last term in Eq. 9—and thus the wall temperatures T_{wi} (i = 1, ..., 6)—possesses an uncertainty of ±0.2K at low heat fluxes up to ±0.5K at the highest heat fluxes in the experiments.

The average Nusselt number based on the heat transfer coefficient is given by

$$Nu = \frac{h_m D_h}{k_b}, \tag{10}$$

where k_b is the thermal conductivity of the static suspension. In terms of Eq. 6, the average Nusselt number is written as

$$Nu = \frac{QD_h}{NA\Delta T_m k_b}. \tag{11}$$

4.2 Error analysis

In order to estimate the heat loss to the environment, a series of single-phase tests was conducted within the same flow rate range. A comparison between electrical power input and water enthalpy increase during the single-phase tests showed that the heat loss is at most about 4%.

According to Eqs. 6 and 11, the errors accounting for h and Nu result from the errors of Q, H_{ch}, W_{ch}, ΔT_m and k_b, which are given in Table 3. Performing the standard error analysis of the corresponding parameters in the study, errors of 6.7 and 9.7% are obtained for h and Nu, respectively.

$$\frac{\delta h}{h} = \left[\left(\frac{\delta Q}{Q}\right)^2 + \left(-\frac{\delta H_{ch}}{H_{ch}}\right)^2 + \left(-\frac{\delta W_{ch}}{W_{ch}}\right)^2 + \left(-\frac{\delta \Delta T_m}{\Delta T_m}\right)^2\right]^{\frac{1}{2}}, \tag{12}$$

$$\frac{\delta Nu}{Nu} = \left[\left(\frac{\delta Q}{Q}\right)^2 + \left(-\frac{\delta H_{ch}}{H_{ch}}\right)^2 + \left(-\frac{\delta W_{ch}}{W_{ch}}\right)^2 + \left(-\frac{\delta \Delta T_m}{\Delta T_m}\right)^2 + \left(-\frac{\delta k_b}{k_b}\right)^2\right]^{\frac{1}{2}}. \quad (13)$$

5 Experimental results and discussions

Heat transfer experiments were conducted using suspensions with MEPCM mass concentrations ranging from 0 to 20%, mass flow rates from 0.05 to 0.35 kg/min and averaged wall heat fluxes ranging from 1.923 to 9.615 W/cm^2, respectively. The applied wall heat fluxes were configured in such a way that they were theoretically able to increase the outlet temperatures of the suspensions for all runs above the endset point of the phase change, i.e., theoretically the suspended MEPCM particles may all undergo complete phase change in the test section. For all runs, the inlet temperatures of the suspensions were kept at 24°C, which is close to the phase change onset point of the used MEPCM.

5.1 Wall temperatures of the minichannels

Figure 7a–d shows the bottom wall temperatures of the minichannels in flow direction for different flow conditions. Due to some heat loss to the outlet port, the wall temperature decreases at the end of the channels. One can see that the wall temperatures strongly depend on the mass flow rate and the MEPCM mass concentration.

For the case of the minimum mass flow rate 0.05 kg/min with a wall heat flux of 1.923 W/cm^2 (Fig. 7a), the wall temperatures decrease as the MEPCM mass concentration increases. The wall temperatures for the suspension with a mass concentration of 5% are 1.0–1.8°C lower than those for water. This temperature reduction increases to 2.5–3.0°C for the 10% suspension and to 4.6–5.5°C for the 20% suspension. Obviously, the suspension with the mass concentration 20% shows the best cooling performance.

Table 3 Measurement errors and manufacturing tolerance

Parameters	Maximum errors	Parameters	Maximum errors
Q	4.0%	ΔT_m	5.3%
H_{ch}	±0.01 mm	k_b	7.0%
W_{ch}	±0.01 mm	h	6.7%
M	0.9%	Nu	9.7%
T	± 0.3°C		

For the case of a mass flow rate of 0.15 kg/min with a wall heat flux of 3.846 W/cm^2 (Fig. 7b), the 5% suspension shows the best cooling performance with the lowest wall temperatures, and the wall temperatures for the 10% and the 20% suspension are between those of water and the 5% suspension. However, the wall temperatures at a certain position in flow direction are close together for all suspensions, and the biggest difference is less than 3°C.

For the case of a mass flow rate of 0.25 kg/min with a wall heat flux of 7.69 W/cm^2 (Fig. 7c), the 5% suspension shows a slightly better cooling performance than water with wall temperatures which are about 1°C lower. However, for higher concentrated suspensions, the wall temperatures increase rapidly with increasing MEPCM concentration. The 20% suspension shows the highest wall temperatures, more than 7°C higher than those of water.

For the case of the maximum mass flow rate of 0.35 kg/min with a wall heat flux of 9.615 W/cm^2 (Fig. 7d), the 5% suspension still shows a better cooling performance than water, with lower wall temperatures by about 2.6°C. For suspensions with a higher mass concentration, the cooling performance becomes again worse. Compared with water, the wall temperatures are more than 3°C higher for the 10% suspension and more than 9°C for the 20% suspension at the position with the highest wall temperature.

The 5% suspension always shows a better cooling performance than water, and for higher concentrated suspensions the cooling performance depends on the mass flow rate. To explain the dependence of the cooling performance of MEPCM suspensions on mass flow rate and MEPCM mass concentration, it is supposed that: (1) The residence time of the suspended MEPCM particles in the channel is longer for a lower mass flow rate, and the MEPCM particles have more time to undergo phase change while flowing through the channel. For example, at M = 0.05 kg/min, the mean residence time of the MEPCM particles is about 4.36 s, but it is only 0.63 s at M = 0.35 kg/min. It is very likely that the phase change in most MEPCM particles has either not yet started or is at least not completed within this short time. Therefore, in such cases the effect of the phase change on the heat transfer is limited. (2) On the other hand, a higher MEPCM mass concentration leads to a decrease of thermal conductivity and sensible heat capacity. Since in a laminar flow heat transfer perpendicular to the flow direction takes place only by conduction, this decrease of thermal conductivity with increasing MEPCM mass concentration deteriorates the heat transfer to the core region of the flow. (3) There are two counteracting effects on the

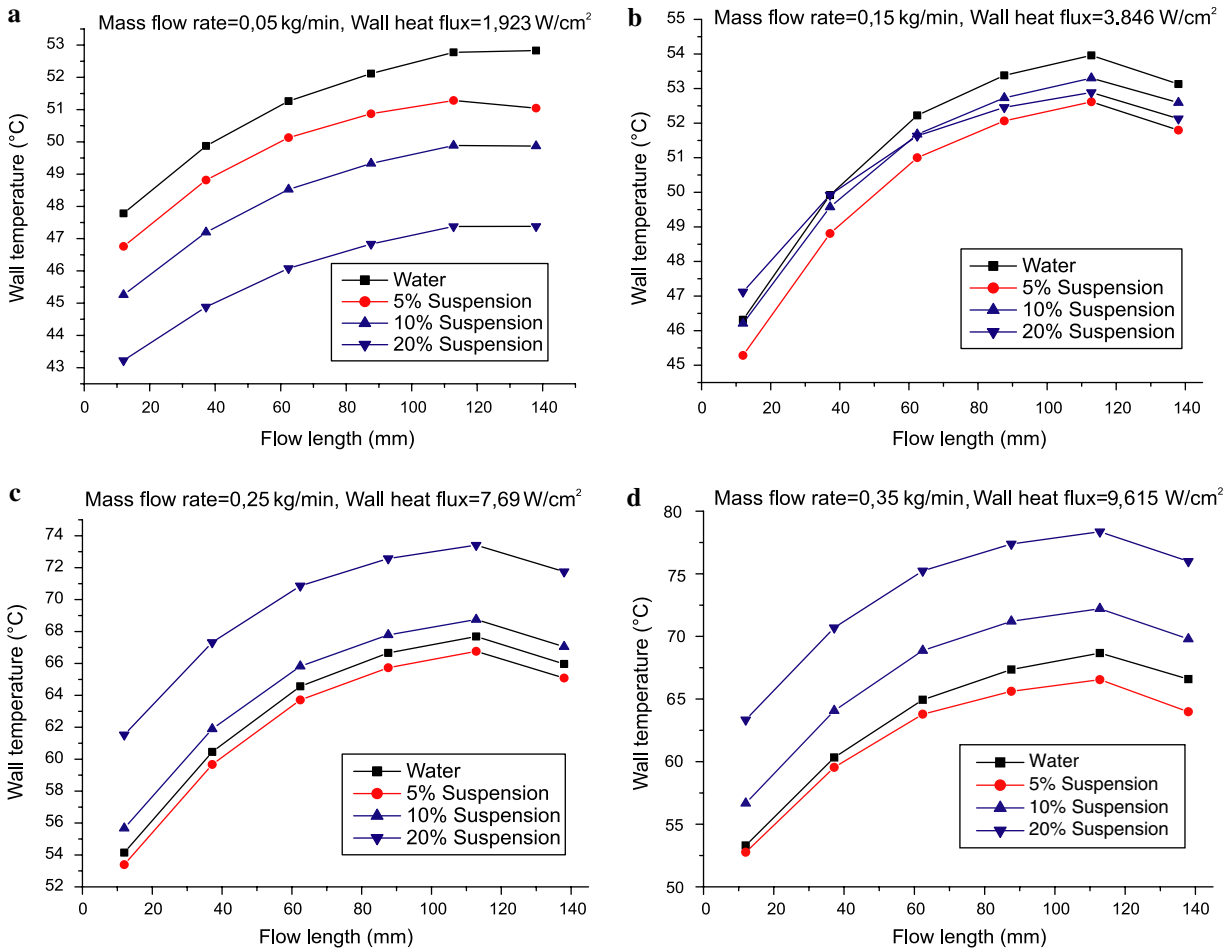

Fig. 7 Wall temperatures of minichannels for MEPCM suspensions of various mass concentrations (T_{in} = 24°C)

cooling performance with increasing MEPCM concentration in the suspension: increasing the heat capacity and decreasing the thermal conductivity. Since the heat transport from the wall to the flow core region deteriorates with increasing concentration, in order to use also the latent heat of MEPCM particles in the flow core region, a certain channel length is necessary. If for a given mass flow rate and a given concentration the channel is long enough, the first positive effect (increasing heat capacity) predominates. This is for example the case for a mass flow rate of 0.05 kg/min. In this case the cooling performance of the suspensions is better than that of water. However for a mass flow rate of 0.35 kg/min and MEPCM concentrations of 10 and 20% the channel is too short, and then the second negative effect (decreasing thermal conductivity) predominates and the cooling performance of the suspension is worse than that of water. The thermal conductivity of the 5% suspension is close to that of water but even this comparatively small fraction of phase change material leads to a considerably increased heat capacity within the temperature ranges of the experiments. Therefore the 5% suspension shows a slightly better cooling performance than water within the whole range of mass flow rates.

5.2 Temperature rise in the suspensions

Figure 8 shows the measured temperature rise between inlet and outlet in the suspensions versus the MEPCM mass concentration. One can see that the temperature rise decreases with increasing MEPCM mass concentration. In the case of the smallest mass flow rate 0.05 kg/min, mainly due to the long residence time of the MEPCM particles in the channel, enough heat is transferred to the core region of the flow and stored as latent heat in the particles. For the mass concentration 20%, the measured temperature rise of the suspension (19.4°C) deviates only 4.4% from the theoretically estimated temperature rise (18.5°C), which is based on the assumption that all the available latent heat is used. For the highest mass flow rates 0.25 and 0.35 kg/min,

mainly due to a shorter residence time of the MEPCM particles in the channel, not much heat is transferred to the core region of the flow and the latent heat of the particles is less efficiently used. For the mass concentration 20% the measured temperature rise of the suspension deviates from the theoretical estimation by 22.5 and 17.6% for M = 0.25 kg/min and M = 0.35 kg/min, respectively. The measured temperature rise is unusually high for the mass flow rate 0.15 kg/min and the MEPCM mass concentrations 10 and 20%. For 20% the measured value (13.9°C) deviates 56.5% from the theoretical estimation (8.9°C). The authors did not find any reliable explanation for this unusual behavior. Thus, further explorations are necessary.

5.3 Heat transfer coefficient and Nusselt number

Figure 9 shows the mean heat transfer coefficients as a function of the MEPCM mass concentration. Each of the four lines belongs to a certain combination of mass flow rate and heat flux.

Within the whole range of mass flow rates from 0.05 to 0.35 kg/min the 5% suspension always shows a slightly better heat transfer performance than water. For the smallest mass flow rate 0.05 kg/min the heat transfer coefficient increases continually with increasing MEPCM concentration, and, compared with water, it is 3.5% higher for the 5% suspension, 11.3% higher for the 10% suspension and 17.1% higher for the 20% suspension. For M = 0.15 kg/min the heat transfer coefficient tends to decrease with increasing mass concentration from 5 to 20%. For the higher mass flow rates 0.25 and 0.35 kg/min the heat transfer coefficient decreases abruptly when the mass concentration is increased from 10 to 20%. Figure 9 also shows that the heat transfer coefficient increases with increasing mass flow rate for all MEPCM mass concentrations. However, this increase in heat transfer coefficient is less distinctive as the MEPCM suspensions become more concentrated and as the mass flow rate becomes bigger.

As Eq. 11 shows, the Nusselt number is closely related to the heat transfer coefficient and to the thermal conductivity of the respective MEPCM suspension. Equation 3 and Table 1 show that the thermal conductivity of the MEPCM suspension decreases with increasing MEPCM mass concentration. Figure 10 shows the mean Nusselt number for the same flow and thermal conditions as in Fig. 9. For the mass flow rate 0.05 kg/min the Nusselt number increases distinctively with increasing MEPCM mass concentration. Compared with water, the Nusselt number is 9.5% higher for the 5% suspension, 19.7% higher for the 10% suspension and 46.5% higher for the 20% suspension. For M = 0.15 kg/min, the Nusselt number tends to increase slowly as the mass concentration increases. For M = 0.25 kg/min and M = 0.35 kg/min, the Nusselt numbers still increase a little bit from water to 5% suspension, but decrease distinctively for greater mass concentrations. Figure 10 also shows that the mean Nusselt number increases with increasing mass flow rate. This increase in Nusselt number becomes less and less distinctive as the MEPCM suspension becomes more concentrated and as the mass flow rate becomes bigger.

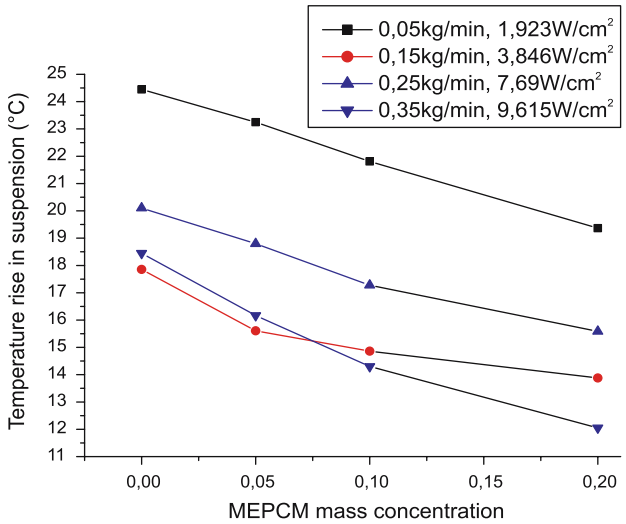

Fig. 8 Temperature rise in the suspensions versus MEPCM mass concentration (T_{in} = 24°C)

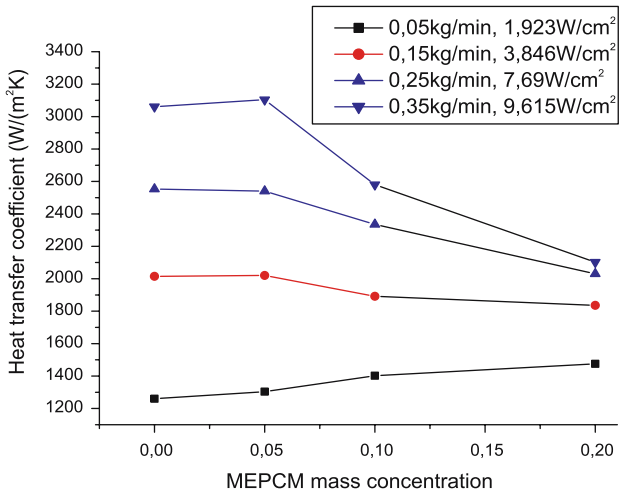

Fig. 9 Mean heat transfer coefficients versus MEPCM mass concentration (T_{in} = 24°C)

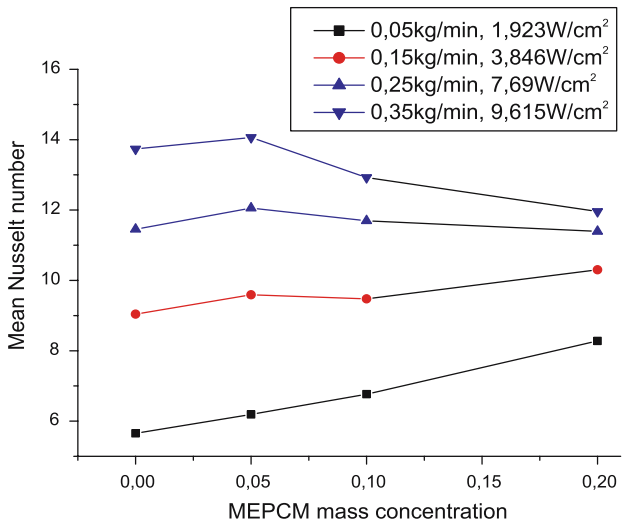

Fig. 10 Mean Nusselt numbers versus MEPCM mass concentration (T_{in} = 24°C)

6 Conclusions

A comparative experimental study has been conducted in order to investigate the laminar flow heat transfer characteristics of MEPCM suspensions flowing through rectangular minichannels. The MEPCM mass concentration ranges from 0 to 20%, and the suspension mass flow rate ranges from 0.05 to 0.35 kg/min. The influences of the MEPCM mass concentration and of the mass flow rate on the heat transfer performance of MEPCM suspensions have been investigated. The following conclusions can be drawn from the experimental study:

1. Mass flow rate and MEPCM mass concentration play a significant role in the cooling performance of MEPCM suspensions. Compared with water, the suspension shows a better cooling performance at a low mass flow rate, i.e., M = 0.05 kg/min. The reduction in wall temperature rise is more distinctive (up to ca. 11%) as the MEPCM mass concentration increases, and the heat transfer coefficient and the Nusselt number increase with increasing mass concentration.
   As the mass flow rate increases, the cooling performance of the MEPCM suspension becomes less and less effective; the wall temperatures are closer to those of a pure water flow or even higher. For each suspension, the heat transfer coefficient and Nusselt number increase with increasing mass flow rate, but this increase becomes less and less distinctive as the MEPCM mass concentration increases.
   It is also found that the suspension with the MEPCM mass concentration 5% always shows a better cooling performance than water by ca. 3% within the whole range of mass flow rates from 0.05 to 0.35 kg/min.

2. It is supposed that the heat transfer performance of suspensions with a higher mass concentration is less effective at higher mass flow rates because of the shorter residence time of the suspended MEPCM particles in the minichannels, the worsened thermal conductivity and less actively moving MEPCM particles in the suspension. This gives some hints how to improve the heat transfer performance of MEPCM suspensions, i.e., optimizing the geometric configuration of the channel, improving the thermal conductivity of the suspension and improving the mixing in the suspension flow.

3. In order to obtain a better cooling performance, suspensions with a higher MEPCM mass concentration are proposed for application at low mass flow rates. Suspensions with a MEPCM mass concentration of less than 10% appear to be more promising for high mass flow rates.

Acknowledgments The author Yu Rao is grateful for the financial support from Deutscher Akademischer Austausch Dienst (DAAD), Chinese Scholarship Council (CSC) and Chinese Natural Science Foundation for his doctoral study. The authors would like to thank Dr. Ekkehard Jahns (BASF AG) for the supply of the MEPCM and helpful discussions, Dr. S. Hardt for the numerical simulation of the flow distribution in the multichannels and Prof. Dr. M. Wilhelm for his help with the rheological investigations.

References

1. Kasza KE, Chen MM (1985) Improvement of the performance of solar energy or waste heat utilization systems by using phase-change slurry as an enhanced heat-transfer storage fluid. J Solar Energy Eng 107:229–236
2. Yamagishi Y, Sugeno T, Ishige T (1996) An evaluation of microencapsulated PCM for use in cold energy transportation medium. In: Proceedings of the 31st intersociety energy conversion engineering conference, IECEC 3:2077–2083
3. Goel M, Roy SK, Sengupta S (1994) Laminar forced convection heat transfer in microcapsulated phase change material suspensions. Int J Heat Mass Transfer 37(4):593–604
4. Inaba H, Kim MJ, Horibe A (2004) Melting heat transfer characteristics of microencapsulated phase change material slurries with plural microcapsules having different diameters. J Heat Transfer 126:558–565
5. Choi E, Cho YI, Lorsch HG (1994) Forced convection heat transfer with phase-change-material slurries: turbulent flow in a circular tube. Int J Heat Mass Transfer 37(2):207–215

6. Choi M, Cho K (2000) Liquid cooling for a multichip module using Fluorinert liquid and paraffin slurry. Int J Heat Mass Transfer 43:209–218
7. Choi M, Cho K (2001) Effect of the aspect ratio of rectangular channels on the heat transfer and hydrodynamics of paraffin slurry flow. Int J Heat Mass Transfer 44:55–61
8. Datta P, Sengupta S, Roy SK (1992) Natural convection heat transfer in an enclosure with suspensions of microencapsulated phase change materials. ASME Gen Pap Heat Transfer 204:133–144
9. Inaba H, Dai C, Horibe A (2004) Natural convection heat transfer in enclosures with microemulsion phase change material slurry. Heat Mass Transfer 40:179–189
10. Vand V (1945) Theory of viscosity of concentrated suspensions. Nature 155:364–365
11. Ward SG, Whitmore RL (1950) Studies of the viscosity and sedimentation of suspensions. Part 1: The viscosity of suspension of spherical particles. Br J Appl Phys 1(11):286–290
12. Campbell GA, Forgacs G (1990) Viscosity of concentrated suspensions: an approach based on percolation theory. Phys Rev A 41:4570–4573
13. Dames B, Morrison BR, Willenbacher N (2001) An empirical model predicting the viscosity of highly concentrated, bimodal dispersions with colloidal interactions. Rheol Acta 40:434–440
14. Gradeck M, Fagla BFZ, Baravian C, Lebouche M (2005) Experimental thermomechanic study of Newtonian and non-Newtonian suspension flows. Int J Heat Mass Transfer 48:3469–3477
15. Zhang Y, Hu H, Kong X (1996) Phase-change energy storage-theoretics and applications. China Science and Technology Press, Hefei, China
16. Technical data from MatWeb-Online Material Data Sheet (2006)
17. Charunyakorn P, Sengupta S, Roy K (1991) Forced convection heat transfer in microencapsulated phase change material slurries: flow in circular ducts. Int J Heat Mass Transfer 34:819–833
18. Sohn CW, Chen MM (1981) Microconvective thermal conductivity in disperse two-phase mixture as observed in a laminar flow. J Heat Transfer 103:47–51
19. Wu HY, Cheng P (2003) An experimental study of convective heat transfer in silicon microchannels with different surface conditions. Int J Heat Mass Transfer 46:2547–2556
20. Qu W, Mudawar I (2003) Flow boiling heat transfer in two-phase micro-channel heat sinks. I. Experimental investigation and assessment of correlation methods. Int J Heat Mass Transfer 46:2755–2771